THE JOURNAL OF CHEMICAL PHYSICS **126**, 204510 (2007)

Thermally activated delayed fluorescence as a cycling process between excited singlet and triplet states: Application to the fullerenes

Carlos Baleizão and Mário N. Berberan-Santos[a)]
Centro de Química-Física Molecular, Instituto Superior Técnico, 1049-001 Lisboa, Portugal

(Received 17 January 2007; accepted 3 April 2007; published online 31 May 2007)

In efficient thermally activated delayed fluorescence (TADF) the excited chromophore alternates randomly between the singlet and triplet manifolds a large number of times before emission occurs. In this work, the average number of cycles $\bar{n}$ is obtained and is shown to have a simple experimental meaning: $\bar{n}+1$ is the intensification factor of the prompt fluorescence intensity, owing to the occurrence of TADF. A new method of data analysis for the determination of the quantum yield of triplet formation, combining steady-state and time-resolved data in a single plot, is also presented. Application of the theoretical results to the TADF of [70]fullerenes shows a general good agreement between different methods of fluorescence analysis and allows the determination of several photophysical parameters. © *2007 American Institute of Physics*. [DOI: 10.1063/1.2734974]

I. INTRODUCTION

Two distinct unimolecular mechanisms exist for molecular fluorescence: *prompt fluorescence* (PF) and *thermally activated delayed fluorescence* (TADF).[1,2] In the PF mechanism, emission occurs after $S_n \leftarrow S_0$ absorption and excited state relaxation to S_1. The TADF mechanism takes place *via* the triplet manifold: After excitation and once attained S_1, intersystem crossing (ISC) to the triplet manifold (T_1 or a higher triplet) occurs, followed by a second ISC from T_1 back to S_1, and by fluorescence emission proper. The cycle $S_1 \rightarrow T_1 \rightarrow S_1$ may repeat a number of times before fluorescence emission, as will be discussed in this work. TADF is significant only when the quantum yield of triplet formation (Φ_T) and the quantum yield of singlet formation (Φ_S) are both high.[3] This in turn implies a small energy gap (ΔE_{ST}) between S_1 and T_1, a long T_1 lifetime, and not too low a temperature.[3] For a given fluorophore, TADF is usually much weaker than its PF. Although known for many years, TADF continues to be a rare phenomenon, with a few observations in some xanthene dyes,[1,4,5] aromatic ketones[6,7] and thiones,[8,9] metal porphyrins,[10] and aromatic hydrocarbons.[11–13]

The remarkable photophysical properties of fullerene C_{70}, specifically the Φ_T very close to one, the small ΔE_{ST} gap and the long intrinsic phosphorescence lifetime, lead to the discovery of an exceptionally strong TADF in this molecule.[3] C_{60} (Ref. 14) and some C_{60} derivatives,[15–17] as well as one C_{70} derivative,[18] also exhibit TADF, but to a lesser degree than C_{70}.

Recently, and owing to its unique TADF properties, C_{70} was used as a sensitive probe for both temperature[19] and molecular oxygen.[20]

In this work, the kinetics of TADF is considered in detail, special attention being paid to the decay parameters and to the interconversion of S_1 and T_1 states. In Sec. II B, it is shown that the average number of cycles performed can be related in a simple way to the fluorescence intensity observables. A new method of fluorescence data analysis, combining steady-state and time-resolved observables, is described in Sec. II C. The experimental details are given in Sec. III. In Sec. IV, the developed theory is applied to the experimental study of the TADF of C_{70} and of a C_{70} derivative dissolved in a solid polymer matrix. The main conclusions are presented in Sec. V.

II. THEORY

A. Thermally activated delayed fluorescence kinetics

The simplest model for thermally activated delayed fluorescence in the condensed phases is a three-state system (thus assuming fast decoherence) that can be represented by the following kinetic scheme:

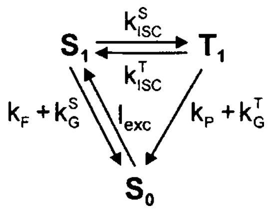

SCHEME 1. Kinetic scheme for TADF.

where $I_{\mathrm{exc}}(t)$ is the excitation intensity, k_F and k_P are the radiative rate constants for fluorescence and phosphorescence, respectively, k_G^S and k_G^T are the nonradiative rate constants for deactivation to the ground state (internal conversion from S_1 and intersystem crossing from T_1, respectively), and k_{ISC}^S and k_{ISC}^T are the ISC rate constants for singlet-to-triplet and triplet-to-singlet conversions, respectively. The triplet-to-singlet ISC rate constant (k_{ISC}^T) is[21–23]

[a)] Electronic mail: berberan@ist.utl.pt

$$k_{\mathrm{ISC}}^{T}(T)=\frac{\Sigma_{v}k_{v}\exp(-E_{v}/k_{B}T)}{\Sigma_{v}\exp(-E_{v}/k_{B}T)}, \tag{1}$$

where k_v is the ISC rate constant of the vth vibrational level of T_1 (v representing the full set of vibrational quantum numbers) and E_v is the respective vibrational energy. Assuming that k_v is a step function, equal to a constant A for $E_v \geqslant \Delta E_{ST}$, where ΔE_{ST} is the S_1-T_1 energy splitting, and zero otherwise, and further assuming that the energy difference between consecutive vibronic levels is much smaller than k_BT, and that the density of states is approximately constant, Eq. (1) becomes the simple Arrhenius equation,[22,23]

$$k_{\mathrm{ISC}}^{T}(T)=A\exp\left(-\frac{\Delta E_{ST}}{k_{B}T}\right), \tag{2}$$

which, owing to the absence of detailed information on k_v and on the density of vibrational states, is the commonly used form for the triplet-to-singlet ISC rate constant. Different assumptions on k_v and on the density of vibrational states lead to a weak temperature dependence of the preexponential factor.[24] Owing to the relative energies of S_1 and T_1, the triplet-to-singlet ISC rate constant always corresponds to an activated process that is strongly temperature dependent.

The time evolution of the S_1 and T_1 populations is given by the following coupled equations,[25] where for simplicity the square brackets representing the concentrations are omitted:

$$S_{1}(t)=I_{\mathrm{exc}}(t)\otimes\exp(-t/\tau_{F})+k_{\mathrm{ISC}}^{T}T_{1}(t)\otimes\exp(-t/\tau_{F}), \tag{3}$$

$$T_{1}(t)=k_{\mathrm{ISC}}^{S}S_{1}(t)\otimes\exp(-t/\tau_{P}), \tag{4}$$

where $\otimes$ stands for the convolution between two functions, $f\otimes g=\int_0^t f(u)g(t-u)du$, $\tau_F=1/(k_F+k_G^S+k_{\mathrm{ISC}}^S)$ is the (prompt) fluorescence lifetime, and $\tau_P=1/(k_P+k_G^T+k_{\mathrm{ISC}}^T)$ is called here the phosphorescence lifetime. These two lifetimes only have direct experimental meaning in the absence of reversibility; otherwise fluorescence and phosphorescence no longer have single exponential decays, as will be discussed below. The low temperature phosphorescence lifetime is $\tau_P^0=1/(k_P+k_G^T)$. In most cases, $k_G^T \gg k_P$. For rigid molecules, the temperature dependence of k_G^T is mainly dictated by external effects, i.e., interactions with the solvent and other solutes present, e.g., oxygen and impurities, and therefore k_G^T is expected to change moderately with temperature in a deoxygenated and photochemically inert solid medium.[26]

Scheme 1 is isomorphous to the monomer-excimer scheme (without transient effects[27]) and has therefore the same general solution. This solution can be obtained by insertion of Eq. (4) into Eq. (3), and then by repeated substitution of the left hand side on the right hand side,

$$S_{1}(t)=I_{\mathrm{exc}}(t)\otimes\exp(-t/\tau_{F})+k_{\mathrm{ISC}}^{S}k_{\mathrm{ISC}}^{T}S_{1}(t)\otimes\exp(-t/\tau_{P})\otimes\exp(-t/\tau_{F}), \tag{5}$$

$$\begin{aligned}S_{1}(t)={}&I_{\mathrm{exc}}(t)\otimes\exp(-t/\tau_{F})+k_{\mathrm{ISC}}^{S}k_{\mathrm{ISC}}^{T}I_{\mathrm{exc}}(t)\\&\otimes\exp(-t/\tau_{F})\otimes\exp(-t/\tau_{P})\\&\otimes\exp(-t/\tau_{F})+(k_{\mathrm{ISC}}^{S}k_{\mathrm{ISC}}^{T})^{2}I_{\mathrm{exc}}(t)\\&\otimes\exp(-t/\tau_{F})\otimes\exp(-t/\tau_{P})\otimes\exp(-t/\tau_{F})\\&\otimes\exp(-t/\tau_{P})\otimes\exp(-t/\tau_{F})+\ldots,\end{aligned} \tag{6}$$

hence the first term for the singlet decay can be associated with prompt fluorescence (zero $S_1\rightarrow T_1\rightarrow S_1$ cycles), and the remaining terms with delayed fluorescence, the nth term resulting from $n-1$ $S_1\rightarrow T_1\rightarrow S_1$ cycles. Analogous results can be obtained for the triplet decay. The singlet decay, Eq. (6), simplifies into a sum of two exponentials of time, and the triplet decay into a difference of the same two exponentials:[28]

$$S_{1}(t)=\frac{S_{1}(0)}{\lambda_{2}-\lambda_{1}}[(\lambda_{2}-X)\exp(-\lambda_{1}t)+(X-\lambda_{1})\exp(-\lambda_{2}t)], \tag{7}$$

where

$$T_{1}(t)=\frac{k_{\mathrm{ISC}}^{S}S_{1}(0)}{\lambda_{2}-\lambda_{1}}[\exp(-\lambda_{1}t)-\exp(-\lambda_{2}t)], \tag{8}$$

with

$$\lambda_{1,2}=\tfrac{1}{2}\{X+Y\mp\sqrt{(Y-X)^{2}+4k_{\mathrm{ISC}}^{S}k_{\mathrm{ISC}}^{T}}\}, \tag{9}$$

$$X=\frac{1}{\tau_{F}}, \tag{10}$$

$$Y=\frac{1}{\tau_{P}^{0}}+k_{\mathrm{ISC}}^{T}. \tag{11}$$

In both TADF kinetics and monomer-excimer kinetics, the intensity of the higher energy emitter (excited singlet state and monomer, respectively) increases with temperature, owing to an increase of the rate of the back step. There is nevertheless one important difference between TADF kinetics and monomer-excimer kinetics: Monomer and excimer intrinsic lifetimes are usually not very different, whereas singlet and triplet excited state intrinsic lifetimes differ by several orders of magnitude. For this reason, the time constants given by Eq. (9) can be simplified in the TADF case to

$$\lambda_{1}=\frac{(1/\tau_{P}^{0})+k_{\mathrm{ISC}}^{T}(1-\Phi_{T})}{1+k_{\mathrm{ISC}}^{T}\tau_{F}}, \tag{12}$$

$$\lambda_{2}=\frac{1}{\tau_{F}}+k_{\mathrm{ISC}}^{T}, \tag{13}$$

where Φ_T is the quantum yield of triplet formation, $\Phi_T = k_{\mathrm{ISC}}^S/(k_F+k_G^S+k_{\mathrm{ISC}}^S)$. It is seen that the fluorescence decay has a short component with a lifetime $1/\lambda_2$ that is smaller than the fluorescence lifetime τ_F, and a long component (delayed fluorescence lifetime) with a lifetime $\tau_{\mathrm{DF}}=1/\lambda_1$ that is smaller than the low temperature phosphorescence lifetime. The higher the temperature, the shorter these two lifetimes are. For $k_{\rm ISC}^T \tau_F \ll 1$, as is usually the case, Eq. (12) reduces to

$$\lambda_1 = \frac{1}{\tau_P^0} + k_{\rm ISC}^T (1 - \Phi_T). \tag{14}$$

This is the form previous used in the literature[3,29] (apart from an incorrect version given earlier in Ref. 28).

It follows from Eq. (7) that the relative amplitude of the long component is

$$C = \frac{\lambda_2 - X}{X - \lambda_1} = k_{\rm ISC}^T \tau_F, \tag{15}$$

and it is always smaller than $A\tau_F$. In the high temperature limit, and assuming that $k_{\rm ISC}^T \tau_F = A\tau_F \ll 1$ still holds, Eq. (12) becomes

$$\lambda_1 = \frac{1}{\tau_P^0} + A(1 - \Phi_T). \tag{16}$$

If $A \ll 1/\tau_F$, as is the case with the [70]fullerenes studied in this work, the short component lifetime $1/\lambda_2$ is essentially temperature independent.

In the above analysis, it is assumed that a relatively fast equilibration exists among the triplet sublevels that can therefore be treated as a single entity whose intrinsic decay rate is the Boltzmann-weighted average of the sublevel decay rates. It is also assumed that upper triplet states whether do not contribute significantly to the TADF process or can be grouped together with T_1 for the purposes of TADF analysis.

B. Strong TADF: Existence of excited state cycles

1. Reformulation of the problem

For strong TADF to occur, the following inequalities must hold: $k_{\rm ISC}^S \gg k_F + k_G^S$ and $k_{\rm ISC}^T \gg k_P + k_G^T$. In most cases, it is also observed that $k_{\rm ISC}^S \gg k_{\rm ISC}^T$ and $k_G^T \gg k_P$. Interconversion of the singlet and triplet emissive states then occurs many times before photon emission or nonradiative decay can take place. In this way, a preequilibrium between S_1 and T_1 exists and the cycle $S_1 \rightarrow T_1 \rightarrow S_1$ repeats a number of times before fluorescence emission occurs. It is interesting to consider the following question: For a given set of rate constants, how many times is the cycle $S_1 \rightarrow T_1 \rightarrow S_1$ completed on the average, before returning to the ground state? Clearly, for a preequilibrium to exist, this cycling must occur many times. In order to quantitatively answer the above question, and related aspects, it is convenient to present the TADF process as the following sequence:

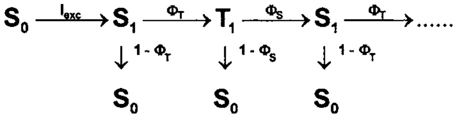

SCHEME 2. Sequential form for TADF.

where the quantum yield of singlet formation is defined by

$$\Phi_S = \frac{k_{\rm ISC}^T}{k_P + k_G^T + k_{\rm ISC}^T}. \tag{17}$$

2. Cycles

One then has

$$\Phi_F = \Phi_{\rm PF}[1 + \Phi_T\Phi_S + (\Phi_T\Phi_S)^2 + \cdots] = \frac{\Phi_{\rm PF}}{1 - \Phi_T\Phi_S}, \tag{18}$$

where the first term corresponds to prompt fluorescence (0 cycle), and the remaining terms correspond to delayed fluorescence, the nth term resulting in general from $n-1$ $S_1 \rightarrow T_1 \rightarrow S_1$ cycles. Equation (18) can also be derived from Eq. (6).

The probability for fluorescence emission to occur after exactly n $S_1 \rightarrow T_1 \rightarrow S_1$ cycles obeys a geometric probability distribution,

$$p_n = (1 - \Phi_T\Phi_S)(\Phi_T\Phi_S)^n. \tag{19}$$

The average number of cycles $\bar{n}$ is thus given by

$$\bar{n} = \sum_{n=0}^{\infty} n p_n = \frac{\Phi_T\Phi_S}{1 - \Phi_T\Phi_S} = \frac{1}{(1/\Phi_T\Phi_S) - 1} = \frac{1}{(1/\Phi_T)(1 + (1/k_{\rm ISC}^T \tau_P^0)) - 1}. \tag{20}$$

3. Experimental meaning of the average number of cycles

The fluorescence quantum yield is given by

$$\Phi_F = \Phi_{\rm PF} + \Phi_{\rm DF}, \tag{21}$$

where the quantum yields for prompt ($\Phi_{\rm PF}$) and delayed ($\Phi_{\rm DF}$) fluorescences obey the following relation:[3]

$$\frac{\Phi_{\rm DF}}{\Phi_{\rm PF}} = \frac{I_{\rm DF}}{I_{\rm PF}} = \frac{1}{(1/\Phi_T\Phi_S) - 1}. \tag{22}$$

Comparison of Eqs. (20) and (22) gives immediately

$$\frac{\Phi_{\rm DF}}{\Phi_{\rm PF}} = \frac{I_{\rm DF}}{I_{\rm PF}} = \bar{n}, \tag{23}$$

and, using Eq. (21),

$$\frac{\Phi_F}{\Phi_{\rm PF}} = \frac{I_F}{I_{\rm PF}} = 1 + \bar{n}, \tag{24}$$

hence the increase in fluorescence intensity owing to TADF is a direct measure of the average number of $S_1 \rightarrow T_1 \rightarrow S_1$ cycles performed. This result is easy to understand, as each return from T_1 to S_1 brings a new opportunity for fluorescence emission.

4. Average lifetime

The average fluorescence lifetime, $\bar{\tau}$, is

$$\bar{\tau} = \sum_{n=0}^{\infty} p_n[(n+1)\tau_F + n\tau_P] = (1 + \bar{n})\tau_F + \bar{n}\tau_P. \tag{25}$$

In the absence of reversibility, $\bar{n}=0$ and $\bar{\tau}=\tau_F$. On the other hand, for the fastest possible excited state equilibration ($k_{\rm ISC}^T \rightarrow A, \Phi_S \simeq 1$), one has

$$\bar{n} \simeq \frac{1}{(1/\Phi_T) - 1}. \tag{26}$$

Therefore, the maximum possible fluorescence intensification factor, Eq. (24), is $1/(1-\Phi_T)$.

The average fluorescence lifetime becomes, as also follows from Eq. (12),

$$\bar{\tau} \simeq \frac{\tau_F}{1-\Phi_T} = \frac{1}{k_F + k_G^S}, \tag{27}$$

which is higher than τ_F, as the ISC channel of S_1 is effectively removed (there is a return to S_1 after every ISC to T_1). The dependence of $\bar{\tau}$ with k_{ISC}^T (and with $\bar{n}$) is nevertheless not monotonic: it increases at first, goes through a maximum for

$$\bar{n} = \frac{1}{\sqrt{1-\Phi_T(1+(\tau_F/\tau_P^0))}} - 1 \simeq \frac{1}{\sqrt{1-\Phi_T}} - 1, \tag{28}$$

where $\tau_P^0 = 1/(k_P + k_G^T)$ is the low temperature phosphorescence lifetime, and then decreases asymptotically to the value given by Eq. (27). The maximum average fluorescence lifetime is approximately given by

$$\bar{\tau} \simeq \left[\frac{2}{\Phi_T}(1-\sqrt{1-\Phi_T}) - 1\right]\tau_P^0. \tag{29}$$

It is seen that this maximum value is always lower than τ_P^0 and decreases with a decrease in Φ_T. The fact that the average fluorescence lifetime passes through a maximum can be explained by the fact that as the average number of cycles increases, so does the weight of the long lifetime component (phosphorescence), Nevertheless, there is a concomitant decrease in the phosphorescence lifetime, hence the existence of a maximum as the result of a compromise between two opposing factors. After the maximum, the dependence of the average fluorescence lifetime on $\bar{n}$ is linear,

$$\bar{\tau} = \frac{\tau_P^0}{\Phi_T} - \left(\frac{1}{\Phi_T} - 1\right)\tau_P^0 \bar{n}, \tag{30}$$

as follows from Eq. (25).

The average fluorescence lifetime can also be written in terms of the time constants λ_1 and λ_2,

$$\bar{\tau} = \frac{1}{\lambda_1}\frac{1+(1/C)(\lambda_1/\lambda_2)^2}{1+(1/C)(\lambda_1/\lambda_2)} = \frac{1}{\lambda_1} - \frac{1}{C\lambda_2} + \cdots , \tag{31}$$

where C is given by Eq. (15). Provided C is not too small (that is, for relatively high temperatures), the expansion can be truncated at the lowest order.

More interesting, a simple relation between λ_1 and $\bar{n}$ can be obtained from Eqs. (14) and (20),

$$\frac{1}{\lambda_1} = \tau_{\mathrm{DF}} = \tau_P^0 - \left(\frac{1}{\Phi_T} - 1\right)\tau_P^0 \bar{n}. \tag{32}$$

This relation is the basis for a new method of data analysis that is detailed below.

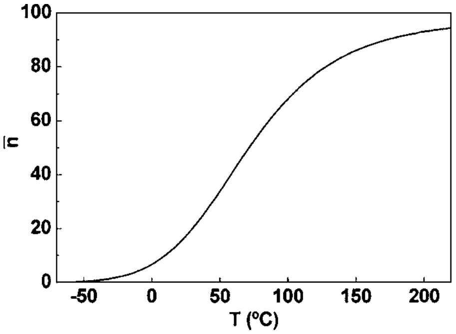

FIG. 1. Average number of $S_1 \rightarrow T_1 \rightarrow S_1$ cycles as a function of temperature for C_{70} in polystyrene.

5. Numerical results

Using the following set of data, obtained in Ref. 19 and in this work for fullerene C_{70} in polystyrene (Sec. IV), $\Phi_T = 0.99$, $\tau_F = 630$ ps, $\tau_P^0 = 28$ ms, $A = 8 \times 10^7\ \mathrm{s}^{-1}$, $\Delta E_{ST} = 29\ \mathrm{kJ\ mol}^{-1}$, estimates of the parameters defined above are obtained: The maximum average number of cycles [Eq. (26)] is predicted to be 99, the limiting fluorescence lifetime [Eq. (27)] to be 63 ns, and the maximum average fluorescence lifetime [Eq. (29)] to be 23 ms, corresponding to an average number of cycles [Eq. (28)] of 9. The computed average number of cycles as a function of temperature is displayed in Fig. 1. It is seen that a large number of excited state cycles are already effected at moderate temperatures. In Fig. 2, the computed average fluorescence lifetime $\bar{\tau}$ and the delayed fluorescence lifetime $\tau_{\mathrm{DF}} = 1/\lambda_1$ are shown as a function of temperature. As expected, they coincide in the moderate to high temperature range, but differ significantly at low temperatures, owing to the reduced importance of TADF in this range, hence the small weight of the long component.

C. Fluorescence data analysis

Several methods of TADF data analysis exist. The classical one, due to Parker,[1] combines steady-state delayed fluorescence and phosphorescence intensities for the determination of ΔE_{ST}. This method was successfully applied to C_{70}.[3] Nevertheless, in many cases it is not possible or convenient to measure the phosphorescence, and it is precisely in these cases that a nonspectroscopic method for the estimation of ΔE_{ST} becomes valuable. Furthermore, photophysical param-

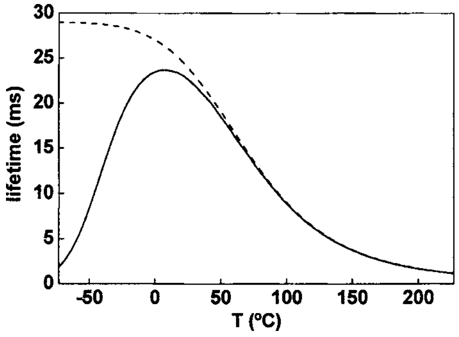

FIG. 2. Average fluorescence lifetime $\bar{\tau}$ (solid line) and delayed fluorescence lifetime τ_{DF} (dashed line) as a function of temperature for C_{70} in polystyrene.

eters other than ΔE_{ST} are of interest and can be extracted from experimental TADF data by other methods. These methods, based exclusively on the measurement of fluorescence, are next discussed.

1. Steady-state data

For the purpose of curve fitting, Eq. (22) can be conveniently rewritten as[3]

$$\ln\left[\frac{I_{\mathrm{PF}}}{I_{\mathrm{DF}}}-\left(\frac{1}{\Phi_T}-1\right)\right]=\ln\left[\frac{1}{\Phi_T}\left(\frac{1}{\Phi_S^{\infty}}-1\right)\right]+\frac{\Delta E_{ST}}{RT}, \quad (33)$$

where

$$\Phi_S^{\infty}=\frac{1}{(1/A\tau_P^0)+1}, \quad (34)$$

and from a fit to steady-state data arranged in the above form,[3] it is possible to recover ΔE_{ST}, Φ_T, and Φ_S^{∞}, assuming that Φ_S^{∞} is temperature independent. Alternatively, a nonlinear curve fitting can also be carried out.

2. Time-resolved data

Using Eq. (2), Eq. (14) becomes

$$\lambda_1=\frac{1}{\tau_P^0}+B\exp\left(-\frac{\Delta E_{ST}}{RT}\right), \quad (35)$$

where $B=(1-\Phi_T)A$. From a nonlinear fit to the temperature dependence of the fluorescence long component (delayed fluorescence lifetime) using Eq. (35), and assuming that τ_P^0 is temperature independent, it is possible to recover ΔE_{ST}, B, and τ_P^0 from time-resolved measurements. Nevertheless, and owing to parameter correlation, it is preferable to fix ΔE_{ST} at the steady-state value [Eq. (33)]. In this way, A and τ_P^0 can be extracted from the temperature dependence of the delayed fluorescence lifetime. Similarly, analysis of the short component given by Eq. (13), rewritten as

$$\lambda_2=\frac{1}{\tau_F}+A\exp\left(-\frac{\Delta E_{ST}}{RT}\right), \quad (36)$$

allows in principle to obtain ΔE_{ST} and A from time-resolved measurements, although the effectiveness of the method depends on the relative importance of the second term, which is usually very small. Bachilo *et al.*[18] used the temperature dependence of the "initial" amplitude of the delayed fluorescence for the evaluation of ΔE_{ST}. While derived in a different way, the basis of the method is simply Eq. (15). The method does not require the assumption that τ_P^0 is temperature independent.

3. Combined steady-state and time-resolved data

A new method of analysis that will be shown here to work well, is the combination of steady-state and time-resolved (delayed fluorescence) data in the same plot according to Eq. (32), rewritten as

$$\tau_{\mathrm{DF}}=\tau_P^0-\left(\frac{1}{\Phi_T}-1\right)\tau_P^0\frac{I_{\mathrm{DF}}}{I_{\mathrm{PF}}}. \quad (37)$$

This linear plot yields Φ_T and τ_P^0, assuming τ_P^0 to be temperature independent. If τ_P^0 is already known, Φ_T can be directly obtained from Eq. (37).

In conclusion, from steady-state and time-resolved data, it is in principle possible to obtain Φ_T, A, ΔE_{ST}, and τ_P^0 using several methods.

III. EXPERIMENT

A. Materials

C_{70} (>99.9%) and polystyrene (PS, average M_w ~280 000, pellets) were purchased from Aldrich[30] and used as received. Toluene (Fluka[30]) was of spectroscopic grade. The methano adduct bis(methyl)-1,2-methano[70]fullerene-71,71-dicarboxylate (1) was synthesized from the reaction of C_{70}, dimethyl malonate, I_2, and DBU as reactants using a modified Bingel procedure.

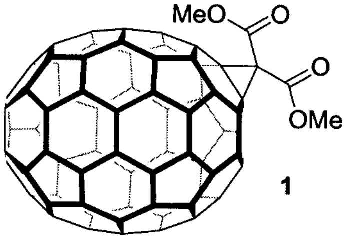

1

CHART 1.

B. Methods

1. Preparation of the films

To prepare the fullerene-containing films (~20 μm thickness), C_{70} or 1 (2.37 mmol) and polystyrene (200 mg) were dissolved in toluene (2 ml), and the mixture was coated onto a quartz plate at room temperature. The plate was introduced into a quartz cell and degassed at room temperature with a turbomolecular pump (final pressure: ~3×10^{-8} atm), and the respective cell sealed afterwards.

2. Spectroscopic measurements

Absorption spectra of fullerenes in PS films and in toluene were recorded on a UV-3101PC UV-visible-NIR spectrophotometer.[31] The fluorescence quantum yields were determined from instrument-corrected spectra using C_{70} in toluene as the standard ($\Phi_F=5.7\times10^{-4}$).[32] Luminescence spectra and time-resolved millisecond fluorescence intensity decays were obtained with a Fluorolog F112A fluorimeter[33] in a front face configuration. Excitation wavelength was 470 nm, and the excitation and emission slits were 18 and 9 nm, respectively. The sample film was mounted slightly away from a 45° angle in order to minimize specular reflection of excitation light. Temperature was controlled to within ±0.5 °C. Time-resolved picosecond fluorescence intensity decays were obtained by the single-photon timing method with laser excitation, with excitation at 470 nm and emission

TABLE I. Fluorescence lifetimes, phosphorescence lifetimes, and fluorescence quantum yields of C_{70} and two monoderivatives.

Compound	τ_F (ns) in toluene	τ_F (ns) in PS	τ_P^0 (ms) at 77 K	$\Phi_F/10^{-4}$ in toluene
C_{70}	0.65[a]	0.63[b]	49 (PS)	5.7[c]
1	0.85	0.84	14 (PS)	9.4
pseudodihydro of C_{70}	1.1[a]	···	6.2[d]	6.2[a]

[a] Reference 38.
[b] Reference 19.
[c] Reference 32.
[d] Reference 37 (7:2 v/v methylcyclohexane-toluene).

at 700 nm. The setup consisted of a mode-locked Innova 400-10 argon-ion laser[34] that synchronously pumped a cavity dumped 701-2 dye laser,[34] delivering 3–4 ps pulses (with ~40 nJ/pulse) at a frequency of 3.4 MHz. Intensity decay measurements were made by alternated collection of impulse and decays with the emission polarizer set at the magic angle position. Impulses were recorded slightly away from excitation wavelength with a scattering suspension. For the decays, a cutoff filter was used to effectively remove excitation light. Detection was always performed by passing the emission through a depolarizer and then through an HR320 monochromator[33] with a grating of 100 lines/mm. Usually no less than 5000 counts were accumulated at the maximum channel. A 2809U-01 microchannel plate photomultiplier[35] served as the detector. Its response function had an effective full width at half maximum of 35 ps.[36] Decay data analysis was performed with the Globals Unlimited software package (Laboratory for Fluorescence Dynamics, University of Illinois, IL).

IV. EXPERIMENTAL RESULTS AND DISCUSSION

A. Absorption and fluorescence

Monofunctionalization of C_{70} brings a slight reduction to the cage π-electronic system and also a lowering of its symmetry and as a result the [70]fullerene derivatives exhibit photophysical properties different from those of C_{70}. The absorption and fluorescence spectra of methano[70]fullerene 1 are similar to those of a 1,2-pseudodihydroderivative of C_{70}.[37,38] Nevertheless, the fluorescence quantum yield is somewhat higher and the fluorescence lifetime slightly shorter, see Table I. Measurements of the prompt fluorescence decays of both compounds between room temperature and 80 °C did not show any variation in the lifetimes.

TABLE II. Photophysical parameters of C_{70} and 1 in PS obtained from the temperature dependence of I_{DF}/I_{PF} according to Eq. (33).

Compound	Φ_T	ΔE_{ST} (kJ mol^{-1})	$-\log \Phi_s^\infty/10^{-7}$	A (s^{-1})
C_{70}	0.99[a]	29[a]	1.285[a]	7×10^7
1	0.96	34	1.124	3×10^8

[a] Reference 19.

The phosphorescence lifetime of 1 is significantly longer than that of 1,2-pseudodihydroderivatives of C_{70},[38] see Table I. The photophysics of 1 remains characterized by a very slow $S_1 \rightarrow S_0$ radiative transition and a fast intersystem crossing as the dominant singlet nonradiative channel, as with the parent fullerene. Incorporation in PS does not change significantly neither the spectra nor the photophysical parameters of the fullerenes, confirming that molecular aggregation is negligible in this medium.

B. Temperature dependence of prompt and delayed fluorescences

1. *Steady-state intensities*

The experimental and fitted values of I_{DF}/I_{PF} as a function of the temperature (between 25 and 90 °C for 1 or 100 °C for C_{70}) are plotted in Fig. 3 for C_{70} and 1 in PS, according to the function [see Eq. (33)],

$$\frac{I_{DF}}{I_{PF}} = (a + b e^{c/T})^{-1}, \tag{38}$$

where

$$a = \frac{1}{\Phi_T} - 1, \tag{39}$$

$$b = \frac{1}{\Phi_T}\left(\frac{1}{\Phi_S^\infty} - 1\right), \tag{40}$$

and

$$c = \frac{\Delta E_{ST}}{R}. \tag{41}$$

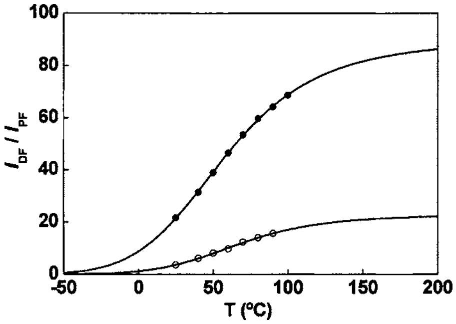

FIG. 3. I_{DF}/I_{PF} as a function of temperature for C_{70} (●) and 1 (○) in polystyrene.

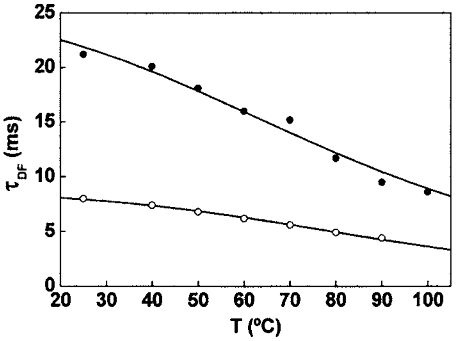

FIG. 4. τ_{DF} as a function of temperature for C_{70} (●) and 1 (○) in polystyrene.

TABLE III. Photophysical parameters of C_{70} and 1 in PS obtained from the temperature dependence of τ_{DF} according to Eq. (35).

Compound	τ_P^0 (ms)	A (s^{-1})
C_{70}	26	8×10^7
1	8.6	2×10^8

Data fitting yields the photophysical parameters given in Table II. The frequency factor A is computed from Φ_S^∞ and from the low temperature phosphorescence lifetimes τ_P^0 given in Table I. The triplet quantum yield of C_{70}, 0.99, is very close to that measured earlier in a liquid alkane,[3] while the effective ΔE_{ST} value of 29 ± 2 kJ mol^{-1} agrees, within experimental error, with earlier determinations.[3,18] The triplet quantum yield value of 0.96, obtained for the methano[70]fullerene 1, represents the first accurate determination made on a C_{70} derivative and is in agreement with the previous finding of $\Phi_T > 0.81$ for a 1,2-pseudodihydroderivative of C_{70}.[38] For this same derivative, a ΔE_{ST} of 30 kJ mol^{-1} was evaluated from the absorption and emission spectra.[38] The present determination of $\Delta E_{ST} = 34\pm2$ kJ mol^{-1} for 1 indicates a higher singlet-triplet energy gap in this compound. We note that an upper limit for the triplet quantum yield is given by $1-\Phi_F$, which is 0.9994 for C_{70} and 0.9991 for 1. These values should be compared with the determined ones, 0.990 ± 0.005 for C_{70} and 0.960 ± 0.005 for 1. Internal conversion is thus the second most important decay channel for S_1 in the case of compound 1, $\Phi_{IC} \approx 0.04$.

2. Delayed fluorescence lifetime

The delayed fluorescence lifetimes (τ_{DF}) of C_{70} and 1 in PS were measured between 25 and 90 °C (1) or 100 °C (C_{70}), and are plotted in Fig. 4. Nonlinear curve fitting according to Eq. (35) and with ΔE_{ST} fixed at the steady-state value (Table II) yields the photophysical parameters given in Table III. The delayed fluorescence lifetimes of 1 are always smaller than those of C_{70}, keeping the order observed at 77 K for the phosphorescence lifetimes. The low temperature lifetimes obtained from the fits (Tables III and IV) are lower but of the same order of magnitude of the phosphorescence lifetimes directly determined (Table I). This means that the phosphorescence lifetime is not perfectly constant, but somewhat decreases with temperature. The effect is nevertheless a minor one when fitting data under the influence of TADF, as the major effect on the delayed fluorescence lifetime is TADF itself, and not the relatively small decrease of the phosphorescence lifetime with temperature. The frequency factors A compare well with those given in Table II and obtained from steady-state data, and are significantly lower than those expected on the basis of detailed balancing,[18] probably as a result of the role of low lying higher triplet states in the intersystem crossing process originating from S_1.

TABLE IV. Photophysical parameters of C_{70} and 1 in PS obtained from a combined steady-state and lifetime analysis according to Eq. (37).

Compound	τ_P^0 (ms)	Φ_T
C_{70}	28	0.99
1	9.2	0.97

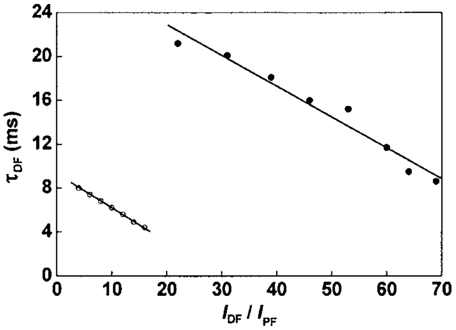

FIG. 5. Linear curve fitting according to Eq. (37) for C_{70} (●) and 1 (○) in polystyrene.

3. Combined steady-state and delayed fluorescence lifetime data analysis

Linear curve fitting according to Eq. (37), shown in Fig. 5, yields the photophysical parameters given in Table IV. The data sets display good linearity. Additionally, the recovered parameters compare very well with those obtained from the methods of analysis already used above. It is thus concluded that the method of analysis based on Eq. (37) gives satisfactory results. This method has the advantage of being linear and of not requiring to presetting the value of any parameter.

V. CONCLUSIONS

In efficient thermally activated delayed fluorescence (TADF) the excited state alternates randomly between excited singlet and triplet manifolds a large number of times before fluorescence emission. In this work, the average number of cycles $\bar{n}$ was derived and shown to have a simple experimental meaning: $\bar{n}+1$ is the intensification factor for prompt fluorescence intensity, owing to the occurrence of TADF. The maximum possible intensification factor was also obtained as $1/(1-\Phi_T)$, where Φ_T is the quantum yield of triplet formation. A new linear method of data analysis for the determination of the quantum yield of triplet formation, combining steady-state and time-resolved data in a single plot, was also presented. Application of the theoretical results to the measured TADF of [70]fullerenes, whose average number of excited state cycles can exceed 100, showed a general good agreement between different methods of data analysis and allowed the determination of several photophysical parameters. With appropriate modifications, the cycle analysis developed in this work can be applied to other reversible photophysical processes, such as monomer-excimer kinetics (work in progress).

ACKNOWLEDGMENTS

This work was supported by Fundação para a Ciência e a Tecnologia (FCT, Portugal) and POCI 2010 (FEDER) within Project No. POCI/QUI/58535/2004. One of the authors

(C.B.) was supported by a postdoctoral fellowship from FCT (SFRH/BPD/14561/2003).

[1] C. A. Parker, *Photoluminescence of Solutions* (Elsevier, Amsterdam, 1968).

[2] B. Valeur, *Molecular Fluorescence: Principles and Applications* (Wiley-VCH, Weinheim, 2002).

[3] M. N. Berberan-Santos and J. M. M. Garcia, J. Am. Chem. Soc. **118**, 9391 (1996).

[4] S. K. Lam and D. Lo, Chem. Phys. Lett. **281**, 35 (1997).

[5] R. Duchowicz, M. L. Ferrer, and A. U. Acuña, Photochem. Photobiol. **68**, 494 (1998).

[6] M. W. Wolf, K. D. Legg, R. E. Brown, L. A. Singer, and J. H. Parks, J. Am. Chem. Soc. **97**, 4490 (1975).

[7] A. M. Turek, G. Krishnammorthy, K. Phipps, and J. Saltiel, J. Phys. Chem. A **106**, 6044 (2002).

[8] A. Maciejewski, M. Szymanski, and R. P. Steer, J. Phys. Chem. **90**, 6314 (1986).

[9] H. Eisenberger and B. Nickel, J. Chem. Soc., Faraday Trans. **92**, 733 (1996).

[10] S. Yusa, M. Kamachi, and Y. Morishima, Photochem. Photobiol. **67**, 519 (1998).

[11] J. L. Kropp and W. R. Dawson, J. Phys. Chem. **71**, 4499 (1967).

[12] B. Nickel and D. Klemp, Chem. Phys. **174**, 297 (1993).

[13] B. Nickel and D. Klemp, Chem. Phys. **174**, 319 (1993).

[14] F. A. Salazar, A. Fedorov, and M. N. Berberan-Santos, Chem. Phys. Lett. **271**, 361 (1997).

[15] M. N. Berberan-Santos, F. A. Salazar, J. M. M. Garcia, C. Santos, T. Fonseca, M. J. M. Curto, and B. Gigante, in *Recent Advances in the Chemistry and Physics of Fullerenes and Related Materials*, edited by K. M. Kadish and R. S. Ruoff (ECS, Pennington, 1998), Vol. 6, p. 319.

[16] B. Gigante, C. Santos, T. Fonseca, M. J. M. Curto, H. Luftmann, K. Bergander, and M. N. Berberan-Santos, Tetrahedron **55**, 6175 (1999).

[17] S. M. Anthony, S. M. Bachilo, and R. B. Weisman, J. Phys. Chem. A **107**, 10674 (2003).

[18] S. M. Bachilo, A. F. Benedetto, R. B. Weisman, J. R. Nossal, and W. E. Billups, J. Phys. Chem. A **104**, 11265 (2000).

[19] C. Baleizão, S. Nagl, S. M. Borisov, M. Schäferling, O. S. Wolfbeis, and M. N. Berberan-Santos, Chem.-Eur. J. **13**, 3643 (2007).

[20] S. Nagl, C. Baleizão, S. M. Borisov, M. Schäferling, M. N. Berberan-Santos, and O. S. Wolfbeis, Angew. Chem., Int. Ed. **46**, 2317 (2007).

[21] H. Kono, S. H. Lin, and E. W. Schlag, Chem. Phys. Lett. **145**, 280 (1988).

[22] H. Fukumura, K. Kikuchi, K. Koike, and H. Kokubun, J. Photochem. Photobiol., A **42**, 283 (1988).

[23] F. Tanaka, M. Okamoto, and S. Hirayama, J. Phys. Chem. **99**, 525 (1995).

[24] Assuming for instance a constant density of states and a single level ISC rate constant given by, $k_v=k_0\exp[-\alpha(E_v-\Delta E_{ST})]$ for $E_v\geqslant\Delta E_{ST}$, and by $k_v=0$ for $E_v<\Delta E_{ST}$, then the ISC rate constant becomes $k_{\mathrm{ISC}}^{T}(T)=\frac{k_0}{1+\alpha k_BT}\exp\left(\frac{-\Delta E_{ST}}{k_BT}\right)$.

[25] M. N. Berberan-Santos and J. M. G. Martinho, Chem. Phys. **164**, 259 (1992).

[26] W. E. Graves, R. H. Hofeldt, and S. P. McGlynn, J. Chem. Phys. **56**, 1309 (1972).

[27] M. N. Berberan-Santos and J. M. G. Martinho, J. Chem. Phys. **95**, 1817 (1991).

[28] J. B. Birks, *Photophysics of Aromatic Molecules* (Wiley, London, 1970).

[29] T. M. Jovin, M. Bartholdi, W. L. C. Vaz, and R. H. Austin, Ann. N.Y. Acad. Sci. **366**, 176 (1981).

[30] www.sigmaaldrich.com

[31] www.shimadzu.com

[32] B. Ma and Y.-P. Sun, J. Chem. Soc., Perkin Trans. 2 **2**, 2157 (1996).

[33] www.jobinyvon.com

[34] www.cohr.com

[35] www.hamamatsu.com

[36] A. A. Fedorov, S. P. Barbosa, and M. N. Berberan-Santos, Chem. Phys. Lett. **421**, 157 (2006).

[37] S. Foley, M. N. Berberan-Santos, A. Fedorov, D. J. McGarvey, C. Santos, and B. Gigante, J. Phys. Chem. A **103**, 8173 (1999).

[38] S. Foley, M. N. Berberan-Santos, A. Fedorov, R. V. Bensasson, S. Leach, and B. Gigante, Chem. Phys. **263**, 437 (2001).